IRAQI JOURNAL OF MATERIALS
Volume (5) Issue (3) July-September 2026, pp. 157-164
Published and Sponsored by American Quality for Scientific Publishing, Inc. (AQSP)

Effects of Reinforcing Material Content on Physical Properties of C-Al-Si-Ti Coatings Prepared by Flame Spray Technique

Maha A. Shaker*, Ali I. Salih

Department of Physics, College of Science, University of Kirkuk, Kirkuk, IRAQ
* Corresponding author email: scpm24004@uokirkuk.edu.iq

Abstract
In this work, the flame spray technique was used to deposit coatings of C-Al-Si-Ti reinforced with different contents of Fe-Cr alloy on stainless steel surfaces to protect them from due to continuous exposure to mechanical stresses and high temperatures. Spray parameters, mainly spray angle of 90°, spray distance of 15-20 cm between the gun nozzle and the substrate, particle velocities approaching 100 m/s according to manufacturer specifications , and a melting point exceeding 1200°C, were controlled to develop more homogeneous and dense microstructures. The hardness of the coated surfaces was found to increase, whereas both porosity and water adsorption decreased, indicating an improvement in coating adhesion and a reduction in structural defects. This behavior is attributed to increased interfacial thermal resistance and microstructural heterogeneity induced by Fe-Cr addition. Therefore, an optimal ratio of reinforcing material was determined to achieve a balance between mechanical strength and thermal efficiency, making these coatings promising candidates for engineering applications operating in harsh environments requiring high resistance to thermal stresses.

***Keywords*:** Flame spray; Physical properties; Cermet coatings; Fe-Cr alloy
Received: April 2026; **Revised:** May 2026; **Accepted:** June 2026; **Published:** July 2026

1. Introduction

Material surface degradation occurs under severe service conditions, where the combined effects of temperature and mechanical loading accelerate deterioration even in resistant alloys such as stainless steel. This makes surface modification an essential approach to maintain long-term performance in advanced engineering materials applications, particularly in environments requiring high resistance to heat, and cyclic stresses [1]. Thermal spray coatings have been adopted as an effective solution, with flame spraying being one of the most attractive techniques due to its simplicity and flexibility in processing a wide range of materials, whether metallic, ceramic, or composite. The properties of the resulting coatings are largely determined by their microstructure, which is controlled during the deposition process. This microstructure directly influences porosity, inter-particle bonding, phase distribution, and consequently the overall coating performance [2]. Therefore, understanding the relationship between processing conditions and microstructure is a fundamental aspect of advanced materials engineering.

The flame thermal spray system represents an integrated setup that combines a thermal energy source, a feedstock delivery system, gas flow control, and the primary deposition tool represented by the spray gun. The importance of this system extends beyond simply generating heat; it also governs the melting state of the material, particle velocity, and trajectory, all of which are critical factors in determining the resulting microstructure. Thus, this system serves as a link between material design and final functional performance [2,3]. The spray gun is considered the core component of this system, playing a crucial role in transforming the feedstock into fine molten or semi-molten particles and propelling them toward the substrate surface. Its importance lies in controlling particle distribution, impact angle, and flattening behavior upon collision which leads to the formation of the so-called lamellar structure. This structure consists of stacked layers of flattened particles (splats), which ultimately determine the final properties of the coating such as density, porosity, thermal conductivity, and resistance [2,4]. It is well known that coatings produced by thermal spraying are not entirely free of structural imperfections, as they typically contain varying levels of porosity, along with inter-splat boundaries and, in some cases, oxides formed due to interaction with oxygen during spraying. Although these features may be undesirable in certain applications, they play a significant role in defining the thermal and physical behavior of the material, particularly in terms of heat transfer and fluid absorption. Therefore, controlling this microstructure is key to improving coating performance [5]. Flame spraying

was selected due to its simplicity and ability to produce coatings with controlled porosity suitable for this study.

In recent years increasing attention has been given to multi-component systems such as C-Al-Si-Ti coatings due to their ability to provide a balanced combination of mechanical and thermal properties. These systems contribute to enhanced hardness, wear resistance, and thermal stability compared to single-component materials [6]. However, the main challenge lies in controlling the structural imperfections generated during deposition, which may limit the efficiency of these coatings in practical applications. To address these challenges, the use of reinforcing phases has been explored as an effective approach to improve structural cohesion, reduce porosity, and enhance inter-particle bonding. The incorporation of Fe-Cr alloy represents one of the promising strategies in this context due to its favorable properties such as toughness, and its ability to interact with the base matrix to improve the microstructure [7]. Moreover, the difference in physical and chemical properties between Fe-Cr and the base material leads to modifications in solidification and deposition behavior, which directly influence the coating properties. Furthermore, the addition of Fe-Cr affects not only the microstructure but also extends to thermal and physical properties such as thermal conductivity and water absorption. The distribution of this reinforcement within the lamellar structure alters heat transfer pathways and reduces open channels that facilitate fluid absorption. Therefore, studying the effect of Fe-Cr content is essential for understanding the mechanisms of improvement and determining the optimal composition that achieves the best overall performance [8].

2. Experimental Part

Following this, several tests were conducted to determine the physical properties. The thermal diffusivity (α) was measured using Laser Flash Analysis (LFA) while thermal conductivity was calculated using k = α ρ Cp. In addition, Lee's Disc apparatus was used as a comparative method to validate the thermal conductivity results manufactured by Griffin & George. The thermal conductivity (*K*) was calculated according to the following equation:

$$K = \alpha \rho C_p \quad (1)$$

where α represents the thermal diffusivity measured by the LFA apparatus (m²/s), ρ represents the sample density (kg/m³) calculated using Archimedes' immersion method , and Cp represents the specific heat of the sample (J/kg.K) calculated using a differential thermal scanning calorimetry (DSC) [3]

It should be noted that all thermal properties in this study were evaluated under room-temperature conditions (~25°C). The thermal diffusivity (*K*) in Eq. (1) is used as an effective parameter to compare different samples rather than a temperature-dependent measured property. No elevated temperature measurements were performed.

The true density and true porosity were also investigated using Archimedes' immersion method according to standard specifications (ASTM-C 830) to determine porosity values without affecting the properties of these coatings. Samples of the coating layers were used after being removed from the substrate to perform the porosity test. Additionally, the water adsorption rate was tested. The coating's water absorption capacity was calculated by immersing dry samples in distilled water for 24 hours after weighing them dry. The surface water was then removed, and the wet samples were weighed. The percentage of water adsorption was calculated [4] according to the following equation [??]:

$$Water\ Adsorption\ \% = \frac{W_{wet} - W_{dry}}{W_{dry}} \times 100 \quad (2)$$

Prior to deposition, the substrate surfaces were carefully prepared using grit blasting to increase surface roughness and thereby enhance the mechanical interlocking and adhesion strength between the coating and the substrate. During the spraying process, key operational parameters such as stand-off distance, spray angle, and torch traverse speed were strictly controlled and kept constant for all samples to ensure uniform coating thickness and minimize microstructural variations across the prepared specimen. Figure (1) shows the surface preparation process using grit blasting prior to coating deposition [5,8].

Each experimental measurement was repeated at least three times to ensure reproducibility. The reported data represent the average values and the standard deviation was found to be within the instrumental accuracy limits. Figure (1) shows photographically sample preparation procedure including (a) cutting of AISI 304 stainless steel substrate, (b) surface drilling/piercing tool used for sample preparation, (c) grit-blasted substrates after surface roughening, and (d) coated samples after flame spray deposition.

IRAQI JOURNAL OF MATERIALS
Volume (5) Issue (3) July-September 2026, pp. 157-164
Published and Sponsored by American Quality for Scientific Publishing, Inc. (AQSP)

(a) (b) (c) (d)

Fig. (1) Sample preparation and coating stages including steel cutting, surface roughening, and sample condition before and after flame spray deposition

The thermal spray coating process was employed as a fundamental step prior to conducting all subsequent physical and thermal characterizations. In this work, a hand-held flame spray system manufactured by Castolin Eutectic was utilized, which is widely recognized in the field of materials engineering for its reliability in depositing functional coatings under industrial and laboratory conditions [5,6]. The system operates on the principle of controlled combustion of a fuel–oxygen mixture to generate a high-temperature flame capable of melting the feedstock material (in powder or wire form) and accelerating it toward the substrate surface .Upon impact, the molten or semi-molten particles undergo rapid flattening and solidification, forming characteristic lamellar structures known as splats, which progressively build up the coating layer. The system shown in Fig. (2) represents the flame spray thermal coating setup used for material deposition [7]. The base coating consists of a C-Al-Si-Ti multiphase composite system, where carbon (C) acts as a carbonaceous phase within an Al-Si-Ti metallic matrix. The unreinforced (0 wt.% Fe-Cr) sample represents this base composite without any additional reinforcement. The base C-Al-Si-Ti powder used for coating preparation had a particle size range of 75-100 µm, while the Fe-Cr reinforcement powder had a particle size range of 45-75 µm. The reinforcement was added in different weight fractions ranging from 0 to 10 wt.% for systematic investigation of its effect on the coating properties .

The post-heat treatment was carried out in a KSL muffle furnace at 850, 950, and 1050 °C with a holding time of 90 minutes. The samples were then cooled inside the furnace under natural air cooling conditions for 30 min. No controlled cooling rate was applied, and the process was conducted under atmospheric conditions without a protective or inert gas; therefore, oxidation was not specifically controlled but was considered minimal due to the short exposure time. All processing parameters including flame spray conditions, substrate specifications, and surface preparation details are summarized in table (1).

This deposition route resulted in the formation of coatings with a well-defined lamellar microstructure and a controlled level of porosity, which is a critical feature influencing the thermophysical behavior of advanced engineering materials [9,10]. The controlled porosity and layered architecture are particularly important in materials systems designed for thermal applications, as they directly affect thermal transport, mechanical integrity, and overall functional performance. Consequently, the adopted flame spray process represents a robust and industrially relevant technique for the fabrication of high-quality coatings in advanced materials research.

Fig. (2) Photographs of the flame spray gun used in this work

ISSN (print) 2958-8960 (online) 3006-6042 Printed in IRAQ

IRAQI JOURNAL OF MATERIALS
Volume (5) Issue (3) July-September 2026, pp. 157-164
Published and Sponsored by American Quality for Scientific Publishing, Inc. (AQSP)

Table (1) Summary of processing parameters

Parameter	Experimental Details
Feedstock	C-Al-Si-Ti base powder (75-100 μm) and Fe-Cr reinforcement powder (45-75 μm), commercially supplied fine irregular powders, mechanically blended in different weight ratios before flame spraying.
Flame spray	Oxygen pressure was 0.7 bar and acetylene pressure was 4.0 bar, with an oxygen-to-acetylene ratio of approximately 1.2:1 to ensure a neutral flame The powder feed rate was experimentally adjusted within a range of 5-15 g/min depending on spraying conditions.
Substrate	The substrate was AISI 304 stainless steel with dimensions of 3 mm thickness and 10 mm diameter. The surface was grit-blasted prior to coating to enhance adhesion; however, the surface roughness was not quantitatively measured
Heat treatment	Preheating at 160-170 °C for 25 min; post-heat treatment at 850-1050 °C for 90 minutes in KSL muffle furnace to reduce porosity and enhance bonding.
Coating thickness	The coating thickness was controlled by spray parameters and was assumed to be in the range of 200-250 μm, consistent with previously reported flame-sprayed composite coatings.
Sample size	Six specimens were used for each experimental condition, and the results were statistically evaluated using average values and standard deviation analysis.

3. Results and Discussion

Figure (3) shows the relationship between Fe-Cr reinforcement content and the effective thermal conductivity (W/m·K) of the coated samples after heat treatment. The results indicate an inverse relationship between Fe-Cr content and thermal conductivity. The unreinforced sample (0% Fe-Cr) exhibited the highest effective thermal conductivity, reaching approximately 170 W/m·K under the present processing conditions. This behavior may be associated with the relatively higher continuity of heat-transfer paths, lower interfacial scattering, and reduced obstruction to phonon and electron transport within the coating structure [11].

With increasing Fe-Cr reinforcement content, the thermal conductivity gradually decreased. At 2% and 4% Fe-Cr, the conductivity decreased to approximately 150 and 130 W/m·K, respectively. Beyond 6% Fe-Cr, the rate of decrease became more gradual, reaching approximately 80 W/m·K at 10% reinforcement. This reduction may be attributed to increased interfacial resistance, phase heterogeneity, and disruption of continuous thermal conduction pathways caused by the addition of Fe-Cr particles [12,13].

All presented values represent average measurements obtained from at least three repeated tests, and the variation remained within acceptable experimental uncertainty.

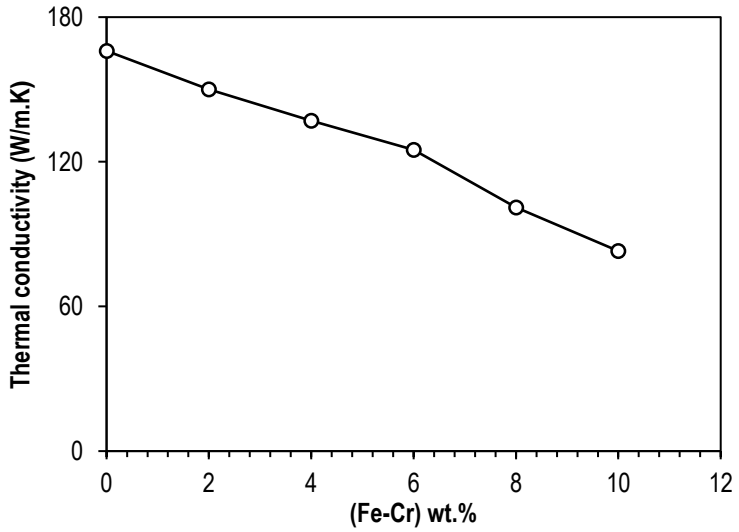

Fig. (3) Effect of reinforcing material content on the thermal conductivity after heat treatment

The reduction in thermal conductivity is mainly attributed to phonon scattering at phase boundaries, inter-splat interfaces and microstructural defects such as porosity and oxide networks Electron scattering plays a secondary role due to the composite and heterogeneous nature of flame-sprayed coatings [14]. It was observed that the main reason for the sharp decrease in heat transfer with the first additions (2% and 4%) is scattering , which means that the electrons lose their thermal energy and

IRAQI JOURNAL OF MATERIALS
Volume (5) Issue (3) July-September 2026, pp. 157-164
Published and Sponsored by American Quality for Scientific Publishing, Inc. (AQSP)

change their directions randomly , which reduces the efficiency of heat transfer in one direction [15]. However, after adding a certain amount of alloying elements (approximately 6% here), we observe a gradual decrease; this is called the saturation zone. At this stage, most of the noise sites on the crystal lattice have been filled with Fe-Cr atoms. Adding more Fe-Cr does not create new defects with the same efficiency but may begin to form discrete phases or atomic clusters. Generally, in flame-sprayed coatings, the effective thermal conductivity is not determined solely by the intrinsic conductivity of the constituent alloys but is primarily determined by micro-defects (porosity, oxide chains, and spray boundaries). Therefore, adding Fe-Cr phase with a low dielectric constant and simultaneously increasing the interfacial/oxide thermal resistance leads to a steady decrease in effective thermal conductivity with increasing Fe-Cr content [16].

Figure (4) shows a direct relationship between increasing the ratio of iron-chromium reinforcing material and increasing the real density. This increase is due to the increased density of the reinforcing material. The heat treatment also contributes to reducing porosity and improving the cohesion of the through thermally induced densification and reduction of internal voids, which helps to increase the density ratio. In some cases, the interaction between the components may lead to the formation of new, denser phases. Thus, it is confirmed that adding the reinforcing material under the applied heat treatment conditions is a successful strategy to improve the real density of the material. This improvement in density is often associated with an improvement in other mechanical properties such as hardness and wear resistance, resulting in a more durable and higher-quality composite material [17,18].

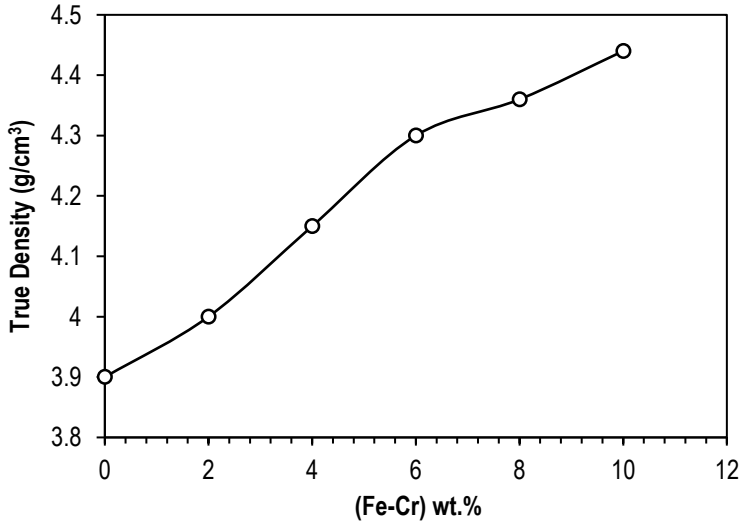

Fig. (4) Effect of reinforcing material content on the true density after heat treatment

Figure (5) illustrates the relationship between Fe-Cr alloy content and the apparent density (g/cm³) of the samples after heat treatment, where the specimens were prepared with different weight fractions (0–10 wt.%). The results show an increasing trend in apparent density with increasing reinforcement content, rising from approximately 3.3 g/cm³ for the unreinforced sample to about 4.2 g/cm³ at 10 wt.% with non-linear gradual increments across intermediate concentrations. This behavior reflects the influence of thermally induced particle bonding and microstructural densification during heat treatment as the addition of Fe-Cr enhances particle bonding and reduces internal porosity leading to a decrease in effective volume and an increase in apparent density. The non-uniform increase in values can also be attributed to the presence of a critical concentration threshold where a certain amount of reinforcement is required to form an effective interconnected structure within the matrix. This was supported by the low experimental deviation of these values [13].

Figure (6) shows the inverse relationship between the addition of the iron-chromium support material and the change in the porosity ratio. We note that when the support material (Fe-Cr) is added to the base material, it acts as a filler, i.e., it fills the interstitial spaces that are formed. This behavior proves that porosity behaves like the filling and bonding theory [19]. In addition to the effect of the heat treatment on the fusion, as the mere presence of the material in the spaces is not enough. Exposure to high temperatures may cause softening and viscous flow of Fe-Cr particles to coat the voids on the surface of the base material. This flow led to the closure of the channels that were connecting the pores to each

other . The observed transition at 6 wt.% represents a microstructural change point inferred from the combined trends of density, porosity, and thermal conductivity. This behavior suggests the formation of a more interconnected reinforcement network within the coating matrix. However, this term is used in a phenomenological sense rather than being confirmed through direct micro-CT or electrical conductivity measurements. This means that the amount of reinforcement material has become sufficient to form a formation of an interconnected microstructural pathway within the coating matrix. This suggests improved particle packing and reduced pore interconnectivity within the coating matrix. The true porosity in this form tells us that the material has become more cohesive and less brittle thanks to the removal of internal weaknesses [21].

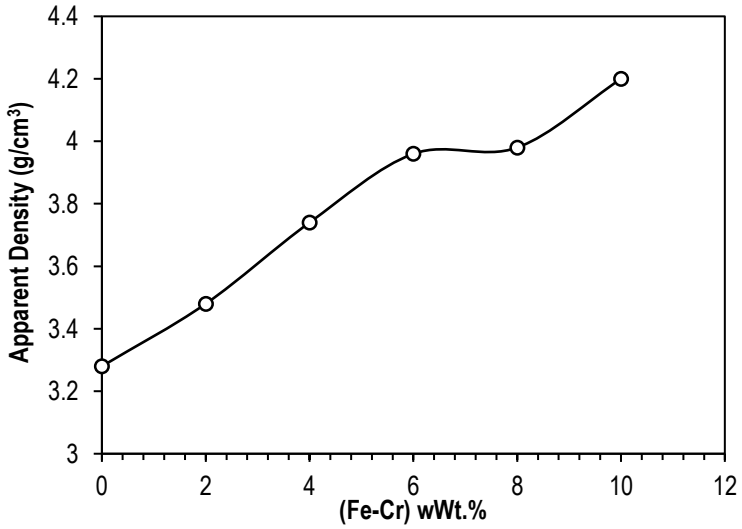

Fig. (5) Effect of reinforcing material content on the apparent density after heat treatment

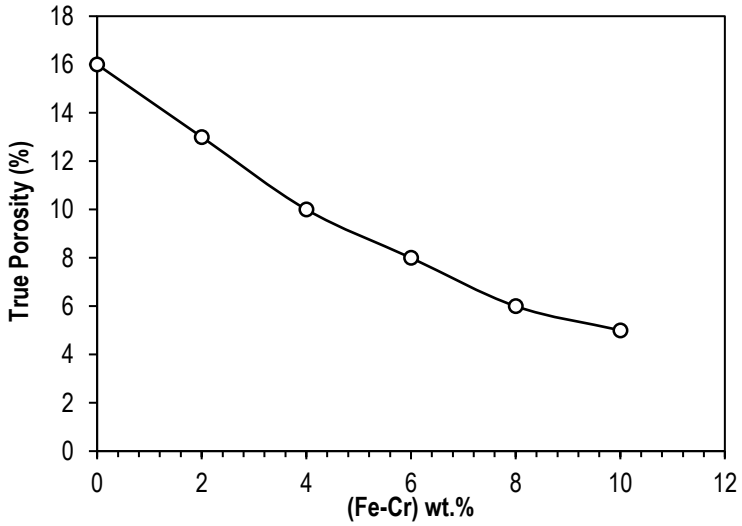

Fig. (6) Effect of reinforcing material content on the true porosity after heat treatment

Figure (7) presents the values of apparent porosity for the prepared coatings at different weight fractions of Fe-Cr alloy after heat treatment, illustrating the effect of coating composition on porosity behavior The horizontal axis represents the reinforcement content (0-10 wt.%) while the vertical axis corresponds to apparent porosity (%), ranging approximately from 13% to 6.2%. The results show an overall decreasing trend in apparent porosity with increasing Fe-Cr content, where it decreases from about 13% for the unreinforced sample to nearly 11% at 2 wt.%, then continues to decrease to 9% at 4 wt.%. The reduction becomes more pronounced at 6 wt.% reaching approximately 8.2% followed by a gradual stabilization at 8–10 wt.% down to about 6.2%.

IRAQI JOURNAL OF MATERIALS
Volume (5) Issue (3) July-September 2026, pp. 157-164
Published and Sponsored by American Quality for Scientific Publishing, Inc. (AQSP)

This behavior is attributed to the combined effect of heat treatment and reinforcement addition where Fe-Cr particles contribute to sealing open pores and reducing pore interconnectivity leading to a decrease in apparent porosity In addition some open pores are transformed into closed pores due to the coverage of surface openings during thermal exposure and particle softening processes, which explains the progressive reduction in porosity values At higher reinforcement contents the effect becomes more stable as the structure approaches a porosity saturation state with a small fraction of fine closed pores remaining that cannot be completely eliminated by conventional processing methods [14].

Figure (8) illustrates an inverse relationship between Fe-Cr content and water absorption behavior, where a significant reduction in water uptake is observed with increasing reinforcement. This behavior is mainly attributed to progressive pore filling and partial pore blocking by the Fe-Cr phase, which reduces the accessibility of open pores to water penetration.

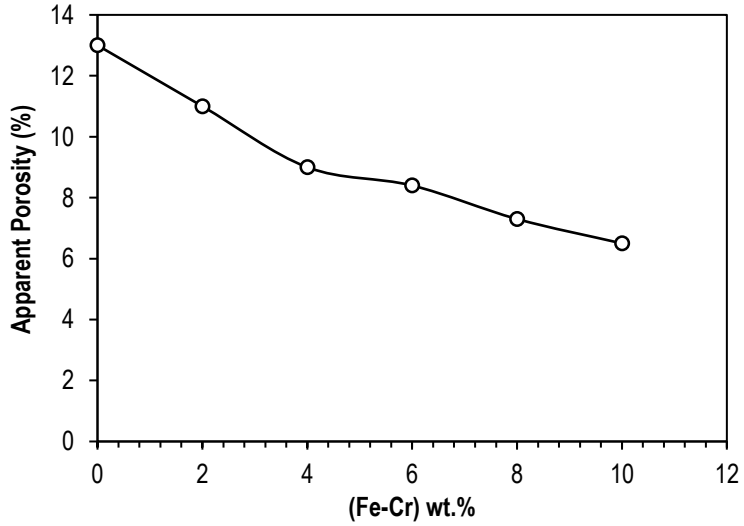

Fig. (7) Effect of reinforcing material content on the apparent porosity after heat treatment

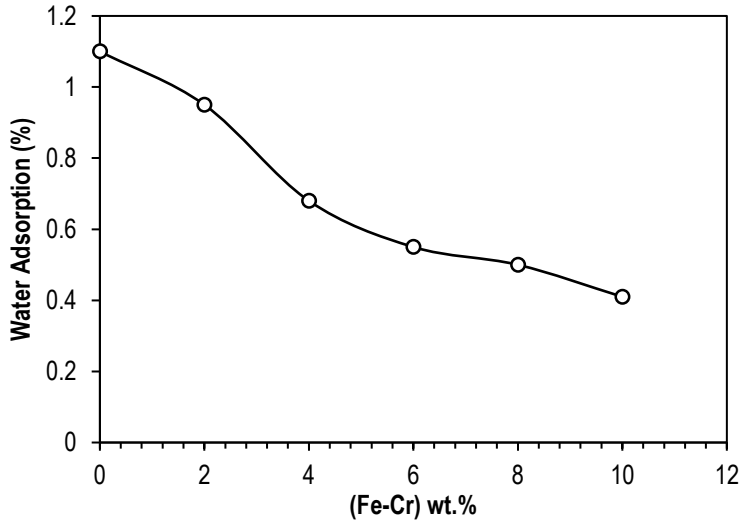

Fig. (8) Effect of reinforcing material content on the water adsorption after heat treatment

At low reinforcement levels (0-4 wt.%), the decrease in water absorption can be associated with partial filling of larger interconnected pores leading to significantly reduced permeability rather than complete impermeability [21]. At intermediate content (around 6 wt.%), further reduction suggests improved densification and reduced pore connectivity within the coating structure. At higher reinforcement levels (8-10 wt.%), the coating exhibits lower apparent porosity, indicating reduced permeability to water ingress.

However, the water absorption does not reach zero, which may be attributed to the presence of fine residual pores and surface adsorption effects. These interpretations are based on the experimental trends of porosity and density measurements rather than direct pore-scale imaging [23]

4. Conclusions

This study showed that the spraying and heat treatment conditions contributed to the formation of a more homogeneous and dense microstructure, which was directly reflected in the improvement of mechanical properties, especially hardness, along with a significant decrease in porosity and water absorption, indicating an increase in coating cohesion and efficiency. It was observed that increasing the Fe-Cr content leads to a decrease in thermal conductivity due to increased interfacial thermal resistance and microstructural heterogeneity within the coating structure. Accordingly, it can be said that choosing an appropriate ratio of reinforcing material is a crucial factor in achieving a practical balance between mechanical strength and thermal efficiency, which serves engineering applications that require high resistance to heat.

References

[1] C. Li et al., "Effects of heat treatment on microstructure and properties of Fe-based amorphous composite coatings", Mater. Sci. Technol., 39(15) (2023) 2168–2178.
[2] L. Pawlowski, "**The science and engineering of thermal spray coatings",** John Wiley & Sons (2008).
[3] F.P. Incropera and D.P. DeWitt, "**Fundamentals of heat and mass transfer**", John Wiley & Sons (2001).
[4] R. Sarkar, "**Refractory Technology: Fundamentals and Applications**", CRC Press (2023).
[5] S.Y. Darweesh, R.A. Rasheed, and M.A. Abdullah, "Treatment of failures in turbine blades by cermet coatings", J. Failure Anal. Prevent., 23(6) (2023) 2461–2470.
[6] M.A. Abdullah, R.Z. Hadi, and S.Y. Darweesh, "Protection of turbine blades by adding metals to ceramic materials using flame coating method", J. King Saud Univ. – Eng. Sci., (2024), doi: 10.1016/j.jksues.2024.02.001.
[7] S.M. Ghareeb, S.M. Aman Allah, S.Y. Darweesh, "Compressive strength, wear, and structure characteristics as a result of silicon carbide addition on a copper base", J. Phys.: Conf. Ser., 1999(1) (2021) 012040.
[8] A.M. Ibrahim, S.M., Aman Allah, and Y.S. Darweesh, "Effect of milling time and boron carbide content on some physical and mechanical properties of an aluminum-based system", AIP Conf. Proceed., 2398(1) (2022) 020046.
[9] L. Pawlowski and P. Fauchais, "Thermal transport properties of thermally sprayed coatings", Int. Mater. Rev., 37(1) (1992) 271–289.
[10] S.H. Humeedi et al., "The effect of adding titanium nanoparticle oxide on the physical properties of nickel by powder method", J. Phys.: Conf. Ser., 1664(1) (2020) 012078.
[11] A. Zhang and Y. Li, "Thermal conductivity of aluminum alloys: A review", *Materials*, 16(8) (2023) 2972.
[12] N. Burger et al., "Review of thermal conductivity in composites: Mechanisms, parameters, and theory", Prog. Polym. Sci., 61 (2016) 1-28.
[13] J. Wang et al., "Development and perspectives of thermal conductive polymer composites", Nanomater., 12(20) (2022) 3574.
[14] R.E.B. Makinson, "The thermal conductivity of metals", Math. Proceed. Cambridge Philo. Soc., 34(3) (1938) 474-497.
[15] J. Appel, "Effect of electron–electron scattering on the electrical and thermal conductivity of metals", Philo. Magaz., 8(90) (1963) 1071-1075.
[16] J. Mascenik and T. Krenicky, "Advanced production, processing, and characterization of industrial materials", Materials, 18(23) (2025) 5366.
[17] D. Wang, H. Zhao, and W. Zheng, "Effect of temperature-related factors on densification, microstructure, and mechanical properties of powder metallurgy TiAl-based alloys", Adv. Powder Technol., 30(11) (2019) 2555-2563.
[18] M. Saleem et al., "Multiferroic materials: Synthesis, properties, and sintering", in **Ferroic Materials: Understanding, Development, and Utilization**, IntechOpen (2025).
[19] G.Y. Koga et al., "An overview of thermally sprayed Fe–Cr–Nb–B metallic glass coatings: From alloy development to coating performance against wear", J. Therm. Spray Technol., 31(4) (2022) 923-955.
[20] M.K. Hassan, "Recent development on fragmentation, aggregation, and percolation", J. Phys. A: Math. Theor., 55(19) (2022) 191001.
[21] L. Łatka et al., "Review of functionally graded thermal sprayed coatings", Appl. Sci., 10(15) (2020) 5153.
[22] A. Ortiz-Marqués et al., "Porosity and permeability in construction materials as key parameters for their durability and performance: A review", Buildings, 15(18) (2025) 3422.
[23] C.N. Adewumi, E.D. Agbaghare, and E.J. Emmanuel, "Kinetics–thermodynamics integration for improved understanding of adsorption mechanisms: A critical perspective", World J. Adv. Res. Rev., 27(2) (2025) 417-443.

